Defence Science Journal, Vol. 68, No. 5, September 2018, pp. 512-518, DOI : 10.14429/dsj.68.12027

Influence of Tool Tilt Angle on Material Flow and Defect Generation in Friction Stir Welding of AA2219

Suresh D. Meshram* and G. Madhusudhan Reddy

DRDO- Defence Metallurgical Research Laboratory, Hyderabad - 500 058, India
**E-mail: suresh_uor@yahoo.co.in*

ABSTRACT

Heat treatable aluminium alloy AA2219 is widely used for aerospace applications, welded through gas tungsten and gas metal arc welding processes. Welds of AA2219 fabricated using a fusion welding process suffers from poor joint properties or welding defects due to melting and re-solidification. Friction stir welding (FSW) is a solid-state welding process and hence free from any solidification related defects. However, FSW also results in defects which are not related to solidification but due to improper process parameter selection. One of the important process parameters, i.e., tool tilt angle plays a critical role in material flow during FSW, controlling the size and location of the defects. Effect of tool tilt angle on material flow and defects in FSW is ambiguous. A study is therefore taken to understand the role of tool tilt angle on FSW defects. Variation in temperature, forces, and torque generated during FSW as a result of different tool tilt angles was found to be responsible for material flow in the weld, controlling the weld defects. An intermediate tool tilt angle (1^o-2^o) gives weld without microscopic defect in 7 mm thick AA2219 for a given set of other process parameters. At this tool tilt angle, x-force, and Z- force is balanced with viscosity and the material flow strain rate sufficient for the material to flow and fill internal voids or surface defects in the weld.

Keywords: Tool tilt angle; Defect; Material flow; Forces

1. INTRODUCTION

Mechanisms occurring during FSW process can be described as follows

(i) Frictional and plastic deformation heating of the base metal beneath the tool shoulder and around the pin
(ii) Transporting the plasticised material ahead of the pin to the back of pin through shear and stirring action
(iii) *In-situ* extrusion combined with forging to consolidate plasticised metal and
(iv) Finally, refilling of the void that is created at the back of pin due to tool movement[1].

The terminology used in FSW is as shown in Fig. 1[2]. The FSW process parameters that mainly control the weld properties (microstructural/mechanical) and defects are tool rotation speed, tool travel speed, tool tilt angle, and tool geometry. Most of the research activity is presently focused towards the effect of tool rotational speed, tool travel speed and tool geometry on mechanical properties and microstructure of the welds. Tool tilt angle, which plays a significant role in controlling the defect in friction stir welds, is studied very scarcely. Tool is tilted in FSW process to:

(i) Avoid the leading edge of the shoulder from removing the material ahead of the tool
(ii) Consolidation of the weld metal at the trailing edge of the tool, and
(iii) Forging action on the material moving from the leading to trailing edge coupled with the plastic deformation heating.

Due to high strength to weight ratio, Al alloy 2xxx series are extensively used in defence and aerospace applications.

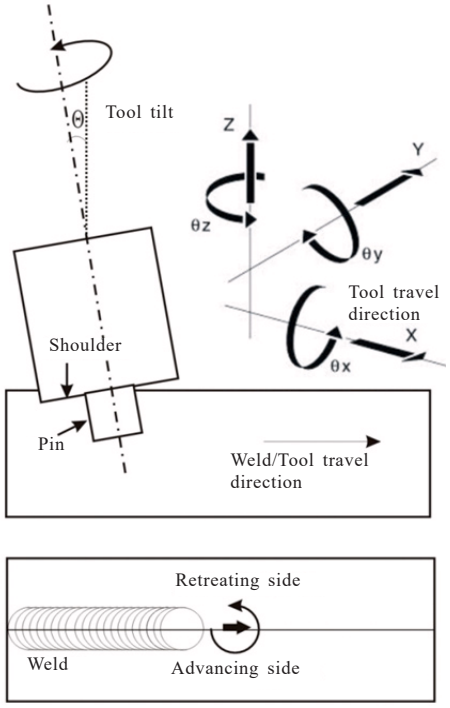

Figure 1. Schematic view of the friction stir welding process and nomenclature[2].

Received : 04 October 2017, Revised : 12 March 2018
Accepted : 26 May 2018, Online published : 12 September 2018

The disadvantage associated with fusion welding of aluminium alloy is mainly due to hydrogen pick-up that causes porosity, oxidation, sensitivity to cracking and, shrinkage[3]. These alloys are therefore mostly joined mechanically through process such as riveting. FSW process is solid-state in nature and hence it is free from solidification related issues mainly associated with the fusion welding process. The ability of FSW process to weld without melting has made most of the aluminium alloys weldable that were considered to be non-weldable earlier, in particular, the 2xxx series alloys. In addition to that FSW also has an advantage over the riveting. FSW welds have greater fatigue strength, weight reduction, and increased structural rigidity as compared to riveted joints[4]. Hence, FSW is considered as an alternative to riveting of Aluminium alloys.

Aluminium alloy AA2219 is a copper containing age-hardenable alloy. AA2219 has a wide range of application that also includes fabrication of liquid cryogenic rocket fuel tanks in defence. It is more commonly used in applications that require high-temperature (within aluminium alloys) and high strength weldments in structural applications[5-8].

Studies on FSW of AA2219 aluminium alloy with respect to the effect of process parameters such as tool rotation speed, tool travel speed, axial load, and tool geometry on microstructural, mechanical and corrosion properties are investigated by many researchers[9-11]. However, the effect of tool tilt angle on material flow behaviour and the consequent effect on joint integrity with respect to defects are not reported. Also, the relationship between tool forces, torque, and temperature experienced by the weld at different tool tilt angle remains unexplored.

It is suggested that tool tilt angle affects the material flow behaviour in the welds during FSW[12]. Investigation of tilt angle on the material flow by Arash[13], *et al.* showed that tool tilt angle is an effective factor in controlling the material flow that also results in imperfection in welds. Effect of tool tilt angle on forces and torque generated during welding of some other aluminium alloys is recently studied but still, the effect of tool tilt angle on defects and material flow is not brought out[14,15]. Long[16], *et al.* studied the effect of tool tilt angle on weld formation, but the correlation of weld defects with material flow strain rate is not covered, though visualisation of material flow is done based on peak temperature experienced by the weld.

Temperature in the weld gives an insight about the material condition (soft/hard) in FSW that helps in visualising the material flow around the tool. Various methods are used by the researchers to measure the temperature of the welds that includes infra-red imaging or with a thermometer in direct contact. These methods have a limitation that only the surface temperature is captured[17] and hence does not gives the information about temperature experienced inside the weld where the defect occurs during FSW. To measure the temperature at the weld nugget, insertion of thermocouple through drilled holes in the plates is required[18]. Material flow behaviour can also be visualised by recording the reaction force on the tool in the direction of tool travel (x-force), along the spindle axis (z-force) and the spindle torque.

In present investigation an attempt is made to understand the effect of tool tilt angle on x-force, z-forces, torque and maximum temperature generated at the weld and the quality (visual and microscopic defects) of the weld. Material flow is analysed based on the observed trend of z-force, x-force, torque, and maximum temperature generated at the weld.

2. EXPERIMENTAL PROCEDURE

The base material used in this study is AA2219-T6, its chemical composition is as shown in Table 1. The base material dimension is 150 mm × 55 mm × 7 mm with square edges. The tool used in this study and its dimensions are as shown in Fig. 2.

Table 1. Chemical composition (wt %) of base metal

Cu	Mn	Si	Zn	Ti	Fe	Zr	Mg	Al
6.7	0.27	0.01	0.04	0.05	0.13	0.12	0.01	Bal

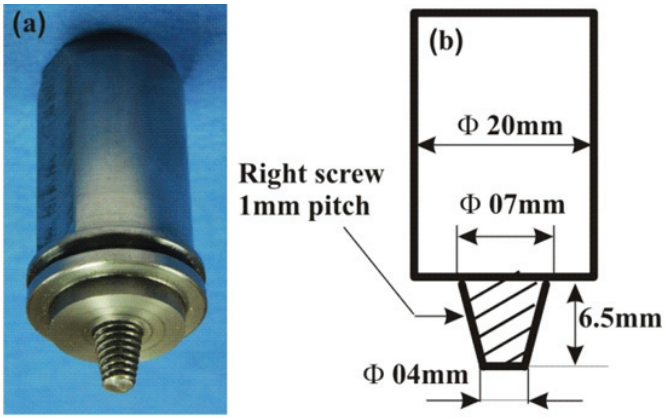

Figure 2. (a) FSW tool and (b) Schematic showing the dimensions of tool.

The tool material used is H13 with hardness 55HRC. The chemical composition of the tool material is given in Table 2. In this investigation, tool rotation speed, tool travel speed, and plunge depth are kept constant at 80 mm/min, 800 rpm and 6.7 mm, respectively based on the initial trials and literature survey[9]. FSW was carried out on a CNC dedicated FSW machine with square butt joint configuration. Keeping the other process parameters constant, the tool tilt angle was varied uniformly from 0° (flat) to 3° at an interval of 0.5° and accuracy of ±0.05. The transverse section of each of the welds was mounted and polished as per standard procedure and etched with Keller's reagent to reveal the macro and microstructures. The temperature at the weld nugget is measured by inserting K-type thermocouple by drilling the hole on either side of the plates to record the temperature on advancing and retracting side (Fig. 3). The temperature generated in the weld is recorded in a data logger with a sampling interval of 10 ms and accuracy of ±2°C for a calibrated K-type thermocouple. The reaction forces and torque are recorded through a multi-axis sensor attached to the spindle head. Three sets of experiments were carried out to ensure the consistency/repeatability of the weld.

Table 2. Chemical composition (wt %) of hot worked die steel (HDS-H13)

C	Cr	V	Mo	Si	Fe
0.30	5.13	1.0	1.33	1.00	Bal.

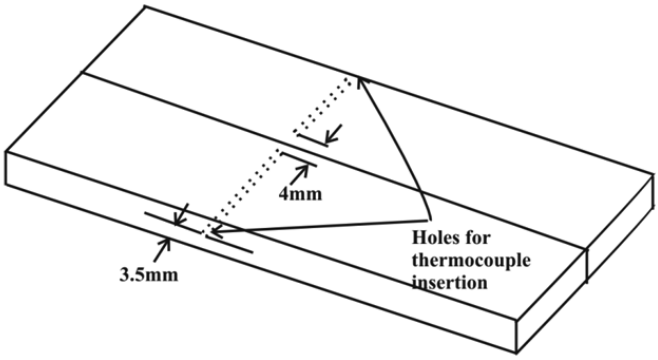

Figure 3. Schematic view of plates with drilled hole for temperature measurement.

The material flow during FSW is driven by the rotating pin. There exists a lag between the rotation speed of the weld metal and that of the pin. By a simple linear assumption so that the average material flow rate (R_m), is about half of the pin rotational speed (R_p) the material flow strain rate, έ, during FSW can be derived by the torsion typed deformation as[19]

$$\varepsilon' = R_m \cdot 2\pi r_e / L_e \quad (1)$$

where r_e and L_e is the effective (or average) radius and depth of the dynamically recrystallised zone (stir zone) respectively as measured from microstructure. The width of the stir zone is taken as radius, and height of the stir zone is the depth of dynamically recrystallised zone as suggested by Chang[19], *et al.* Using Eqn. (1) weld metal flow strain rate at different tool angle is evaluated.

Couette fluid flow model is a mechanistic representation of the material viscosity during material flow between concentric rotating cylinders. The material viscosity is approximated as

$$\mu = \left(r_1^2 - r_0^2\right) M / 4\pi r_1^2 r_0^2 \left(\omega_1 - \omega_0\right) \quad (2)$$

where r_0 and ω_0 are the radius and angular velocity of the inner cylinder while r_1 and ω_1 is radius and angular velocity of the outer cylinder respectively. M is the torque per unit depth of the cylinder[20]. Assuming that thickness of the rotating layer of material around the pin does not vary significantly with varying tool tilt angle, which was also observed during optical microscopy, viscosity (μ) is proportional to torque (M) in Eqn 2. Hence, torque recorded by the spindle transducer represents the viscosity of the material around the pin.

3. RESULTS AND DISCUSSION

3.1 Influence of Tool Tilt on Welds

Top surface image (crown surface) of the welds made at different tool tilt angle is as shown in Fig. 4.

It is observed that with an increase in tool tilt angle from 0° (flat) to 3°, surface defects appear at 0° - 0.5° and beyond 0.5° tilt there is no surface defect. Weld from 0° to 2° does not show any defect when the transverse section was examined under the microscope as shown in Fig. 5. However, welds made at 2.5° and 3° showed internal defects. Weld at 2.5° showed a kissing bond defect which grows into a void at the subsequent increase of tool tilt angle to 3°.

Defects occur in friction stir welds with parameters that results, excessive heating of the weld or insufficient heating of the weld, referred as hot or cold processing condition respectively. Under cold processing with slip conditions between tool and workpiece, insufficient flow of material results in surface lack of filling, wormhole, or lack of consolidation defects on the advancing side[21].

When there is no tool tilt (0°), the material in contact with the shoulder moves in a plane almost parallel to the plane of the shoulder, considering horizontal movement of the weld metal around the tool pin. However, a tilt given to the tool results in pushing the material downward from retreating to advancing side along the trailing edge due to the combined action of rotational and translational movement of the tool. This downward movement of material at the trailing end of the shoulder can be considered as a forging action due to tool tilt angle.

At 0° tool tilt angle, the shoulder is in complete contact with the plate, hence more material is to be transported along the retreating side from leading to trailing edge at the top surface of the weld. Fig. 6 shows the temperature generated during welding with different tool tilt angle. Weld temperature is relatively low at a 0° tool tilt angle. This indicates that weld metal is not softened to the extent essential for the easy and complete transport of the material from leading to trailing edge of the tool. Weld metal flow strain rate computed at 0° tool tilt

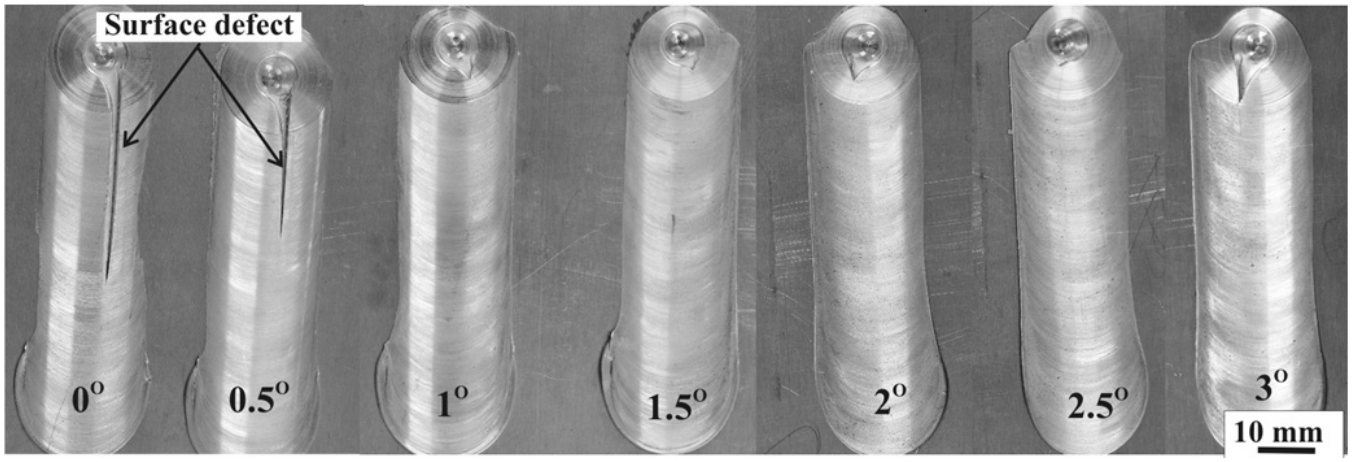

Figure 4. Top surface images of the weld zone with various tool angles.

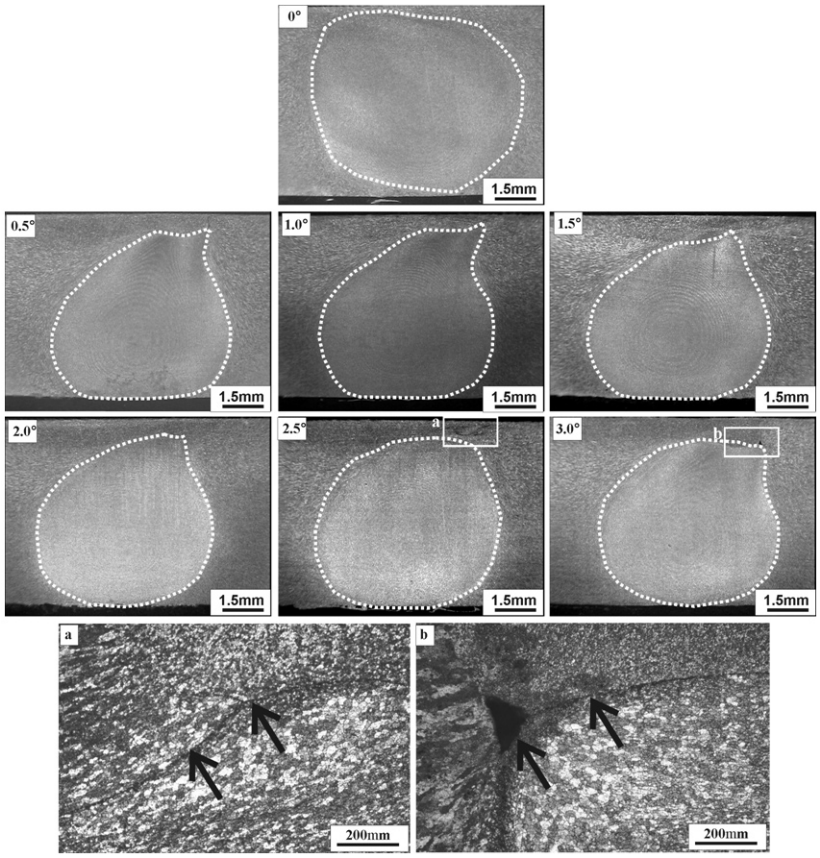

Figure 5. Low magnification images of a transverse section of welds at different tool tilt angle 0°, 0.5°, 1.0°, 1.5°, 2.0°, 2.5°, and 3° with an enlarged view of defect at (a) 2.5° tool tilt angle (b) 3° tool tilt angle.

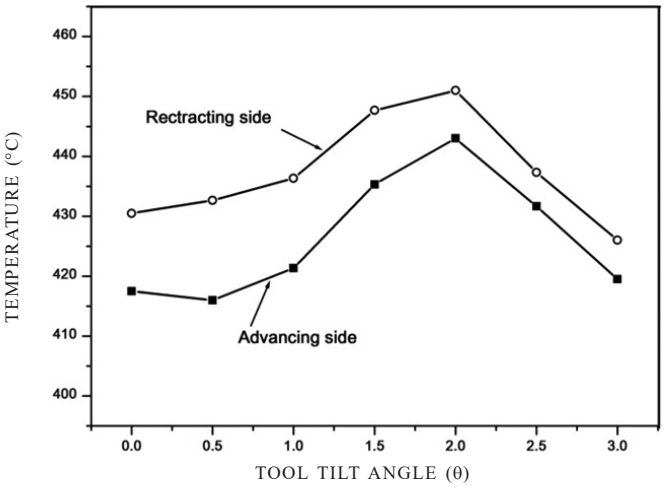

Figure 6. Temperature on advancing and retreating side at different tool tilt angle.

angle, which is low, also confirms the sluggish movement of weld metal as shown in Fig. 7. Similarly, the very high torque value at 0° tool tilt angle indicates that large volume of weld metal with low temperature is transported from leading to trailing edge of the tool as shown in Fig. 8. The low temperature at 0° tool tilt can be attributed to the absence of forging action, which contributes to plastic deformation heating. Low temperature and flow strain rate of weld metal at 0° tool tilt angle, therefore, results insufficient flow of material at the top surface of the weld leading to surface defects. A 0° tool tilt results to defect in the weld is also reported by Long[16], *et al.*.

With increasing tool tilt angle, amount of material to be transported from leading to trailing edge on the top surface of the weld reduces. There is a gradual increase in temperature, because of the plastic deformation heat associated with the forging action of the tool on material beneath. An increase in the temperature brings down the viscosity of the material which is evident from the decrease in the torque experienced by the tool as shown in Fig. 8. The less viscous material gets easily transported along the retreating side which is consistent with the increase in metal flow strain rate values, i.e. the material is moving with high velocity filling the surface defects.

An optimum value is reached between 1° and 2° of tool tilt angle wherein the torque/viscosity of the material, the amount of material transported and the weld metal flow strain rate is sufficient for filling up of surface defects. Derazkola[12], *et al.* and Long[16], *et al.* also demonstrated that 2° tool tilt angle is optimum for getting friction stir welds without defects.

Further increase in tool tilt angle (beyond 2°) results in an insufficient flow of material at the top surface of weld due to the reduction in contact area at the leading edge of the tool between shoulder and workpiece plate. This results in defect below the top surface of the plate on advancing side. These defects start in the form of kissing-bond defects and finally grow into the voids with increasing tool tilt angle (Figs. 5(a) and 5(b). Since higher tool tilt angle results in low contact area at the leading edge, heat generated due to shoulder at the top surface is low, bringing down the overall temperature of the weld. Low temperature results in a higher viscosity of the material that moves around the pin at a low flow strain rate as shown in Fig.7, which is insufficient for filling of the lost material on the advancing side below the surface of weld resulting into defects

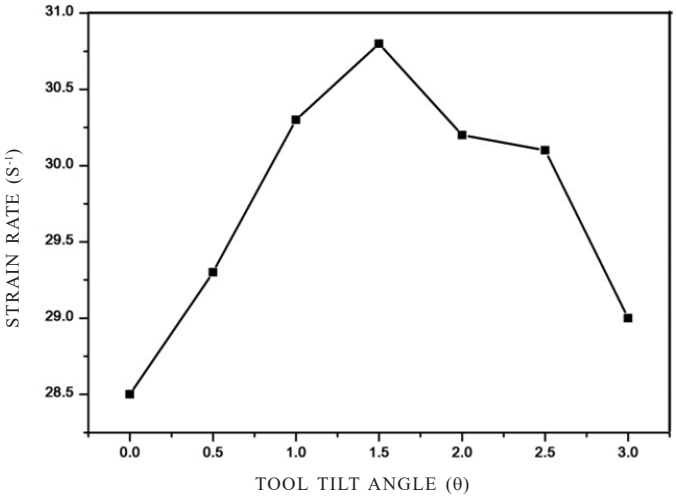

Figure 7. Material flow strain rate calculated at different tool tilt angle.

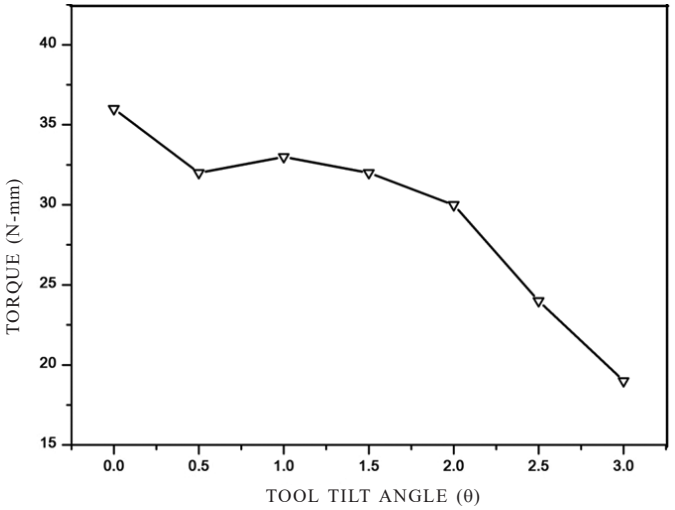

Figure 8. Measured torque at different tool tilt angle.

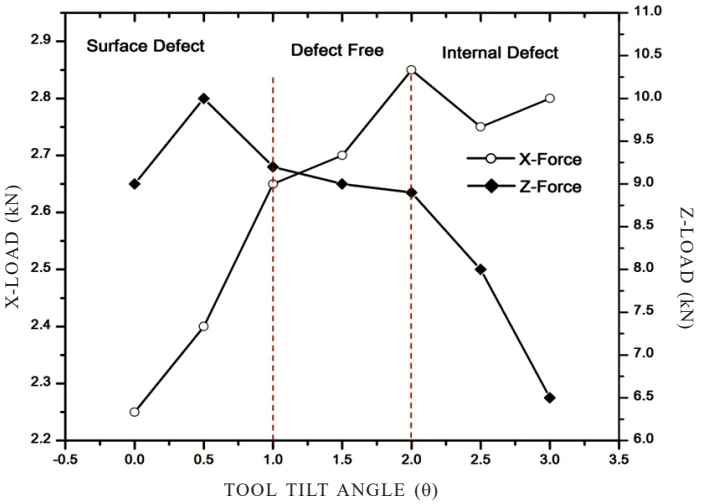

Figure 9. Variation in x-force and z-force at different tool tilt angle.

on advancing side.

Nugget zones are basically classified to be of two types basin-shaped that widens near the upper surface[22] and elliptical nugget[23]. Basin-shaped nuggets are formed when upper surface experience extreme deformation and frictional heating by contact with the cylindrical tool shoulder. Figure 5 shows that weld nugget with 0° tool tilt angle resembles more like a basin-shaped nugget compared to the weld nugget at 2° tool tilt angle which is an elliptical nugget. At a 0° tool tilt angle, the shoulder is in complete contact with the top surface resulting in high frictional heating with extreme deformation at the top surface; a probable cause for a basin-shaped nugget.

Nugget shape is also dependent on the temperature generated in the weld. The shape of the weld nugget is most clearly distinguished when tool rotational speed (rpm) is varied[24]. Low rpm results in basin-shaped nugget as compared to high rpm. The effect of an rpm on temperature is well documented[18] and stated that an increase in rpm results in an increase in temperature of the weld nugget. In the present study it is observed that nugget shape is in conformity the temperature recorded as shown in Fig. 6, i.e. it's more like basin-shaped at low temperature and elliptical at high temperature, except at 0° tool tilt angle for which the reason is discussed previously as shown in Fig. 5. High temperature leads to softening of the material and reduce the size of the deformation region[25].

3.2 Influence of Tool Tilt on x-force (Transverse Force)

FSW tool experiences a transverse force, mainly due to greater reaction force on the front of tool pin, since the temperature of the metal (aluminium) ahead of the tool is lower and has high flow stress as compared to the metal at the trailing edge. Effect of tool tilt angle on x-force which is along the tool travel direction is as shown in Fig. 9. X-force continuously increases with increase in tool tilt from 0° to 3°. This increase in x-force with an increase in tool tilt can be attributed to three factors. The forging action or plunge action at the front portion of the tool continuously reduces with increase in tool tilt angle; resulting in reduced heating of weld metal ahead of the tool pin that intern increases the reaction force on the tool. Secondly, as the tool is tilted, the longitudinal (horizontal) component of the z-force increases and is added up to the x-force[1]. Lastly, with an increase in tool tilt angle the front portion of the tool pin is exposed more to the un-deformed low-temperature material with high flow stress that offers high resistance/reaction force to the motion of the tool in the tool travel direction. Large x-force, therefore, an indication of the sluggish flow of the weld metal around the pin and hence the defects are observed in the form of kissing bonds and voids at higher tool tilt angle[26].

3.3 Influence of Tool Tilt on z-force

There is an increase in the z-force as the tool tilt is changed from a flat position (0°) to a tilt of 0.5° as shown in Fig. 9. When the pin tool is inclined by 0.5° and is moving along the weld line there is an additional component of z-force acting upward, pushing the material up ahead of the pin. It is similar to the "ploughing" action taking place ahead of the pin. This upward force that pushes the material up ahead of the pin must be countered by an additional downward force to maintain a given plunge depth ahead of the pin[27]. The material beneath the shoulder at the front of the pin is harder, as evident from the lower temperature recorded with a tool tilt of 0.5° as shown in Fig. 6, and hence requires higher downward force to maintain the plunge depth. This explains the increase in z-force as the tool tilt is increased from 0 to 0.5°.

Beyond 0.5° tool tilt angle, plunging of the tool at the trailing edge resulting in high frictional heating and softening of the weld metal beneath the shoulder as shown in Fig. 6 and a corresponding decrease in z-force. This phenomenon occurs till the tool tilt of 2°.

At a tool tilt of 1° to 2° moderate z-load is experienced; which is an indication of adequate hydrostatic pressure and temperature generated at the weld that is essential for the consolidation of the weld material to get weld without defects[28]. However, when tool tilt is more than 2° it results in a drastic drop in z-force and temperature, which can be attributed to very low contact of the shoulder in front of the pin. Reduction in weld metal flow strain rate at 2.5° and 3° tool tilt, low weld

metal temperature and z-force all together indicates sluggish movement of material around the pin resulting into formation of internal voids.

4. CONCLUSIONS

Tool tilt angle plays an important role during FSW of AA2219. Tool tilt angle governs the material flow characteristic of the weld, controlling the size and location of the defects. Material flow in the weld with different tool tilt angle can be visualised by observing the temperature generated at the weld, reaction forces and torque experienced by the tool. Correlation of these output parameters with the weld quality (defect size/ location) provides a significant insight into material flow characteristic as a result of tool tilt angle during FSW. For the specified tool geometry, there exists an optimum value of tool tilt angle between 1° to 2° during FSW of 7 mm thick AA2219 below which surface defects occur and beyond 2° internal voids gets developed. At tool tilt angle of 1° to 2° the material is heated to a fully plasticised condition with viscosity, material flow strain rate, x-forces, and z-force attending the value adequate for proper stirring and forging of the weld material giving welds without defect.

REFERENCES

1. Zhang, G.F.; Su, W.; Zhang, J. & Zhang, J.X. Visual observation of effect of tilting tool on forging action during FSW of aluminium sheet. *Sci. Technol. Weld. Join.*, 2011, **16**(1), 87-91. doi:10.1179/136217110X12714217309650
2. Meshram, S.D.; Reddy, G.M. & Venugopal R.A. Role of threaded tool pin profile and rotational speed on generation of defect free friction stir AA 2014 aluminium alloy welds. *Def. Sci. J*., 2016, **66**(1), 57-63. doi: 10.14429/dsj.66.8566
3. Flores, O.V.; Kennedy, C.; Murr, L.E.; Brown, D.; Pappu, S.; Nowak, B.M. & McClure, J.C. Microstructural issues in a friction-stir-welded aluminum alloy. *Scripta Materialia*, 1998, **38**(5), 703-708. doi:10.1016/S1359-6462(97)00551-4
4. Trimble, D.; Monaghan, J. & O'donnell, G.E. Force generation during friction stir welding of AA2024-T3. *CIRP Ann. Manuf. Technol.,* 2012, **61**(1), 9-12. doi:10.1016/j.cirp.2012.03.024
5. Huang, C. & Kou, S. Partially melted zone in Aluminum welds-liquation mechanism and directional soldification. *Welding Journal*, 2000, **79**(5), 113s-120s.
6. Biddle, A.P. & Wilson, W.A. Variable polarity plasma arc welding on the space shuttle external tank. *Welding Journal*, 1984, **63**, 27–35.
7. Albertini, G.; Bruno, G.; Dunn, B.D.; Fiori, F.; Reimers, W. & Wright, J.S. Comparative neutron and X-ray residual stress measurements on Al-2219 welded plate. *Mater. Sci. Eng.: A,* 1997, **224**(1-2), 157-165. doi:10.1016/S0921-5093(96)10546-3
8. Xu, W.; Liu, J.; Luan, G. & Dong, C. Microstructure and mechanical properties of friction stir welded joints in 2219-T6 aluminum alloy. *Materials Design*, 2009, **30**(9), 3460-3467. doi:10.1016/j.matdes.2009.03.018
9. Lakshminarayanan, A.K.; Malarvizhi, S. & Balasubramanian, V. Developing friction stir welding window for AA2219 aluminium alloy. *Trans. Nonferrous Met. Soc. China*, 2011, **21**(11), 2339-2347. doi: 10.1016/S1003-6326(11)61018-2
10. Rambabu, G.; Naik, D.B.; Rao, C.V.; Rao, K.S. & Reddy, G.M. Optimization of friction stir welding parameters for improved corrosion resistance of AA2219 aluminum alloy joints. *Defence Technology*, 2015, **11**(4), 330-337. doi:10.1016/j.dt.2015.05.003
11. Arora, K.S.; Pandey, S.; Schaper, M. & Kumar, R. Microstructure evolution during friction stir welding of aluminum alloy AA2219. *J. Mater. Sci. Technol.,* 2010, **26**(8), 747-743. doi: 10.1016/S1005-0302(10)60118-1
12. Derazkola A.H.. & Simchi, A. Experimental and thermomechanical analysis of friction stir welding of poly (methyl methacrylate) sheets. *Sci. Technol. Weld. Join.*, 2018, **23**(3), 209-218. doi: 10.1080/13621718.2017.1364896
13. Arash, R. & Amir M. Influence of machine parameters on material flow behavior during channeling in modified friction stir channelling, *Int. J. Mater. Form*., 2016, **9**(1), 1-8. doi: 10.1007/s12289-014-1193-8
14. Elyasi, M.; Aghajani, D.H. & Hosseinzadeh, M. Investigations of tool tilt angle on properties friction stir welding of A441 AISI to AA1100 aluminium. Proceedings of the Institution of Mechanical Engineers, Part B: *J. Eng. Manuf*., 2016, **230**(7), 1234-1241. doi: 10.1177/0954405416645986
15. Banik, A.; Roy, B.S.; Barma, J.D. & Saha, S.C. An experimental investigation of torque and force generation for varying tool tilt angles and their effects on microstructure and mechanical properties: Friction stir welding of AA 6061-T6. *J. Manuf. Process.*, 2018, **31**, 395-404. doi: 10.1016/j.jmapro.2017.11.030
16. Long, L. Chen, G.; Zhang, S.; Liu, T. & Shi, Q. Finite-element analysis of the tool tilt angle effect on the formation of friction stir welds. *J. Manuf. Process.*, 2017, **30**, 562-569. doi: 10.1016/j.jmapro.2017.10.023
17. Mahoney, M.W.; Rhodes, C.G.; Flintoff, J.G.; Bingel, W.H. & Spurling, R.A. Properties of friction-stir-welded 7075 T651 aluminum. *Metall. Mater. Trans. A*, 1998, **29**(7), 1955-1964. doi: 10.1007/s11661-998-0021-5
18. Tang, W.; Guo, X.; McClure, J.C.; Murr, L.E. & Nunes, A. Heat input and temperature distribution in friction stir welding. *J. Mater. Process. Manuf. Sci.*, 1998, **7**(2), 163-172. doi:10.1106/55TF-PF2G-JBH2-1Q2B
19. Chang, C.I.; Lee, C.J. & Huang, J.C. Relationship between grain size and Zener-Holloman parameter during friction stir processing in AZ31 Mg alloys. *Scripta Materialia*, 2004, **51**(6), 509-514.

doi:10.1016/j.scriptamat.2004.05.043
20. Crawford, R.; Cook, G.E.; Strauss, A.M.; Hartman, D.A. & Stremler, M.A. Experimental defect analysis and force prediction simulation of high weld pitch friction stir welding. *Sci. Technol. Weld. Join*., 2006, **11**(6), 657-665. doi:10.1179/174329306X147742
21. Arbegast, W.J. A flow-partitioned deformation zone model for defect formation during friction stir welding. *Scripta materialia*, 2008, **58**(5), 372-376. doi:10.1016/j.scriptamat.2007.10.031
22. Sato, Y.S.; Kokawa, H.; Enomoto, M. & Jogan, S. Microstructural evolution of 6063 aluminum during friction-stir welding. *Metall. Mater. Trans. A*, 1999, **30**(9), 2429-2437. doi: 10.1007/s11661-999-0251-1
23. Rhodes, C.G.; Mahoney, M.W.; Bingel, W.H.; Spurling, R.A. & Bampton, C.C. Effects of friction stir welding on microstructure of 7075 aluminum. *Scripta Materialia*, 1997, **36**(1), 69-75. doi:10.1016/S1359-6462(96)00344-2
24. Ma, ZY.; Mishra, R.S.; Mahoney, M.W. Friction stir processing for microstructural modification of an aluminium casting. In Friction stir welding and processing II, edited by Jata, K.V.; Mahoney, M.W, Mishra, R.S, Semiatin, S.L. & Lienert T. TMS, San Diego, US, 2003. pp. 221–230.
25. Colegrove, P.A. & Shercliff, H.R. CFD modelling of friction stir welding of thick plate 7449 aluminium alloy. *Sci. Technol. Weld. Join*., 2006, **11**(4), 429-441. doi:10.1179/174329306X107700
26. Reynolds, A.P.; Tang, W.; Posada, M. & DeLoach, J. Friction stir welding of DH36 steel. *Sci. Technol. Weld. Join.*, 2003, **8**(6), 455-460. doi:10.1179/136217103225009125
27. Melendez, M.; Tang, W.; Schmidt, C.; McClure, J.C.; Nunes, A.C. & Murr, L.E. Tool forces developed during friction stir welding. NASA Technical Reports Server (NTRS), Document ID:20030071631.
28. Kumar, K. & Kailas, S.V. The role of friction stir welding tool on material flow and weld formation. *Mater. Sci. Eng.: A,* 2008, **485**(1), 367-374. doi:10.1016/j.msea.2007.08.013

ACKNOWLEDGMENTS

The authors thank DRDO for the financial support and Dr Vikas Kumar, Director DMRL for his continued encouragement and support.

CONTRIBUTORS

Mr Suresh D. Meshram received BE (Mechanical) from NIT, Surat, in 2000 and MTech (Prod. & Ind. System Engg.) from IIT Roorkee, in 2002. He is working as scientist 'E' at DRDO-Defence Metallurgical Research Laboratory, Hyderabad. His area of research mainly includes joining of advance similar and dissimilar materials through process like electron beam welding, friction welding and friction stir welding and characterisation of welded joints.
Experimentation and data generation is carried out by him in the present study.

Dr G. Madhusudhan Reddy, obtained PhD in Metallurgical Engineering from Indian Institute of Technology, Madras in 1999. As a Scientist 'H' he is heading the metal joining group of DRDO-Defence Metallurgical Research Laboratory, Hyderabad. He has more than 300 scientific publications to his credit. He is a Fellow of the ASME (USA), IWS (India) and Institution of Engineers (India). He has received *Metallurgist of the Year*, *DRDO scientist of the year award*.
Data analysis and correlation of weld defects with different input and output parameters are carried out by him